Magnetic Resonance Studies of SAPO-44 and MnAPSO-44

Zviya Olender (Levi),† Daniella Goldfarb,*,† and J. Batista‡

Contribution from the Department of Chemical Physics, Weizmann Institute of Science, Rehovot 76100, Israel, and Department of Catalysis and Chemical Reaction Engineering, Boris Kidrič Institute of Chemistry, Hajdrihova 19, P.O. Box 30, 61115 Ljubljana, Slovenia.
Received May 18, 1992

Abstract: A variety of magnetic resonance experiments were performed to investigate the local environment of Mn in MnAPSO-44. MnAPSO-44 is a member of the aluminophosphate molecular sieves family and has a chabazite-like structure. Two samples with different Mn contents (Mn/(P + Al + Si) = 0.9 and 0.07 atom %) in their as-synthesized, calcined hydrated and dehydrated forms were studied. The ^{31}P, ^{29}Si, and ^{27}Al MAS NMR spectra are similar to those of the corresponding SAPO-44 samples showing only one type of TO_4 tetrahedra. In the hydrated sample an ^{27}Al signal at −13 ppm, characteristic of octahedral Al, appears as well due to water coordination. EPR spectra were measured at X- and Q-band. The Mn(II) in the as-synthesized and calcined samples showed hyperfine splittings of 85 and 93 G, respectively, the latter being characteristic of octahedral environment. Dehydration at 400 °C reduced the hyperfine constant to 65 G, indicating a change to tetrahedral coordination upon water removal. The nuclei in the immediate surrounding of the Mn were probed by the electron spin echo envelope modulation (ESEEM) technique. Both ^{31}P and ^{27}Al modulations were observed. The EPR and ESEEM results are interpreted in terms of Mn incorporation into tetrahedral framework sites for the sample with the low Mn content. The spatial distribution of the Mn throughout the sample was investigated by the "2 + 1" electron spin echo (ESE) experiment. It was found that only about 15% of the Mn(II) is homogeneously distributed and contributes to the echo signal.

Introduction

The aluminophosphate molecular sieves ($AlPO_4$)[1] have structural characteristics similar to those of zeolites, forming channels and cavities which can host sorbate molecules. A serious drawback of these materials with respect to catalytic potential is the lack of Brönsted acidity due to the neutrality of their framework. This can, however, be overcome by framework substitution of P and/or Al by other elements to generate negatively charged frameworks. One possible substitution is with Si, yielding the silicoaluminophosphate molecular sieves abbreviated as SAPOs.[2] Another possibility is substitution, in both AlPOs and SAPOs, with transition metals such as Co, Ti, Mn, and Fe.[3] The successful incorporation of the transition metals into the framework is, however, in some cases still questionable. Several characterization studies on CoAPO-5 reported that the Co(II) is tetrahedrally coordinated in framework sites both after synthesis and following calcination.[4-6] It was also found that the amount of Co(II) that can be incorporated into the framework of AlPO-5 is very limited, namely, Co/P < 1 atom %.[5,6] Unlike CoAPO-5, most of the Mn(II) in MnAPO-5 was found to be extraframework even at very low Mn(II) contents.[7] Furthermore, the Mn(II) distribution in MnAPO-5 was found to be inhomogeneous, i.e. aggregates of Mn(II) with Mn(II)-Mn(II) distances of 10-15 Å were found.[7] Different Mn(II) local environments in hydrated MnAPO-11 as compared to Mn(II) impregnated onto hydrated AlPO-11 and water coordination typical to Mn(II) occupying a negatively charged site suggest that at low Mn(II) contents, 0.1 mol %, the Mn(II) is incorporated into the framework.[8] Similar results were obtained for MnAPSO-11.[9]

Mn(II) and Co(II) have been incorporated into the chabazite-like structures SAPO-34 and SAPO-44 and the activity and shape selectivity of these materials were tested on methanol dehydration.[10] It was found that both MeAPSO-44 and MeAPSO-34 (Me = Mn,Co) showed better activity than the unsubstituted materials. Moreover, the MeAPSO-44 materials showed considerably better selectivity. The selectivity was found to depend on the substituting element. In this study the Me content was Me/(P + Si) = 2 atom %, which is higher than the Me contents reported for successful incorporation so far. In the present paper we investigate the local environment of the Mn in MnAPSO-44 by NMR and a variety of EPR techniques in order to obtain a better understanding of its activity. We used ^{27}Al, ^{31}P, and ^{29}Si MAS NMR to characterize the materials and to obtain information regarding the Si substitution. The environment of the Mn(II) was followed by X-band and Q-band EPR spectroscopy and electron spin echo envelope modulation (ESEEM) spectroscopy. The ESEEM experiment is most useful in probing weak superhyperfine interactions between the paramagnetic center and neighboring nuclear spins.[11] In this particular case we can use the modulation from framework ^{31}P and ^{27}Al to probe the Mn(II) location.[7] We have also used the "2 + 1" electron spin echo (ESE) experiment[12] to investigate the spatial distribution of the Mn(II). This experiment was specifically designed to study the dipolar interaction between paramagnetic centers which can

Table I. Composition of Materials Studied (Atomic Ratios)

sample[a]	Al	P	Si	Mn
SAPO-44	0.48	0.40	0.12	
	(1.19)[b]	(1.0)	(0.30)	
MnAPSO-44(1)	0.495	0.354	0.142	0.009
	(1.40)	(1.0)	0.40	(0.026)
MnAPSO-44(2)	0.505	0.343	0.151	0.0007
	(1.47)	(1.0)	(0.44)	(0.002)

[a] Obtained from the calcined samples. [b] Relative atomic content normalized to the P content.

† Weizmann Institute of Science. Incumbent of the Charles H. Revson Foundation Career Development award.
‡ Boris Kidrič Institute of Chemistry.

(1) Wilson, S. T.; Lok, B. M.; Messina, C. A.; Cannan, T. R.; Flanigen, E. M. *J. Am. Chem. Soc.* **1982**, *104*, 1146.
(2) Patton, R. L.; Gajeck, R. T.; Cannan, T. R.; Flanigen, E. M. US Patent 4,440,871, 1984.
(3) Flanigen, E. M.; Lok, B. M.; Patton, R. L.; Wilson, S. T. *New Developments in Zeolites Technology*; Murakami, Y., Ijima, A., Ward, J., Eds.; Kodansha: Tokyo, 1986; p 103.
(4) Iton, L. E.; Choi, I.; Desjardins, J. A.; Maroni, V. A. *Zeolites* **1989**, *9*, 457.
(5) Shiralkar, V. P.; Saldariaga, C. H.; Perez, J. O.; Clearfield, A.; Chen, M.; Anthony, R. G.; Donohue, J. A. *Zeolites* **1989**, *9*, 474.
(6) Schoonheydt, R. A.; de Vos, R.; Pelgrims, J.; Leeman, H. *Zeolites: Facts, Figures and Future*; Jacobs, P. A., van Santen, R. A., Eds.; Elsevier: Amsterdam, 1989; p 559.
(7) Levi, Z.; Raitsimring, A. M.; Goldfarb, D. J. *Phys. Chem.* **1991**, *95*, 7830.
(8) Lee, C. W.; Chen, X.; Bronet, G.; Kevan, L. *J. Phys. Chem.* **1992**, *96*, 3110.
(9) Bronet, G.; Chen, X.; Lee, C. W.; Kevan, L. *J. Am. Chem. Soc.* **1992**, *114*, 3720.
(10) Hočevar, S.; Batista, J. *Advances in Catalyst Design*; Graziani, M., Rao, C. N. R., Eds.; World Scientific: Singapore, 1991; p 137.
(11) Kevan, L. In *Time Domain Electron Spin Resonance*; Kevan, L., Schwartz, R. N., Eds.; Wiley-Interscience: New York, 1979; Chapter 8.
(12) Kurshev, V. V.; Raitsimring, A. M.; Tsvetkov, Y. D. *J. Magn. Reson.* **1989**, *81*, 441.

0002-7863/93/1515-1106$04.00/0

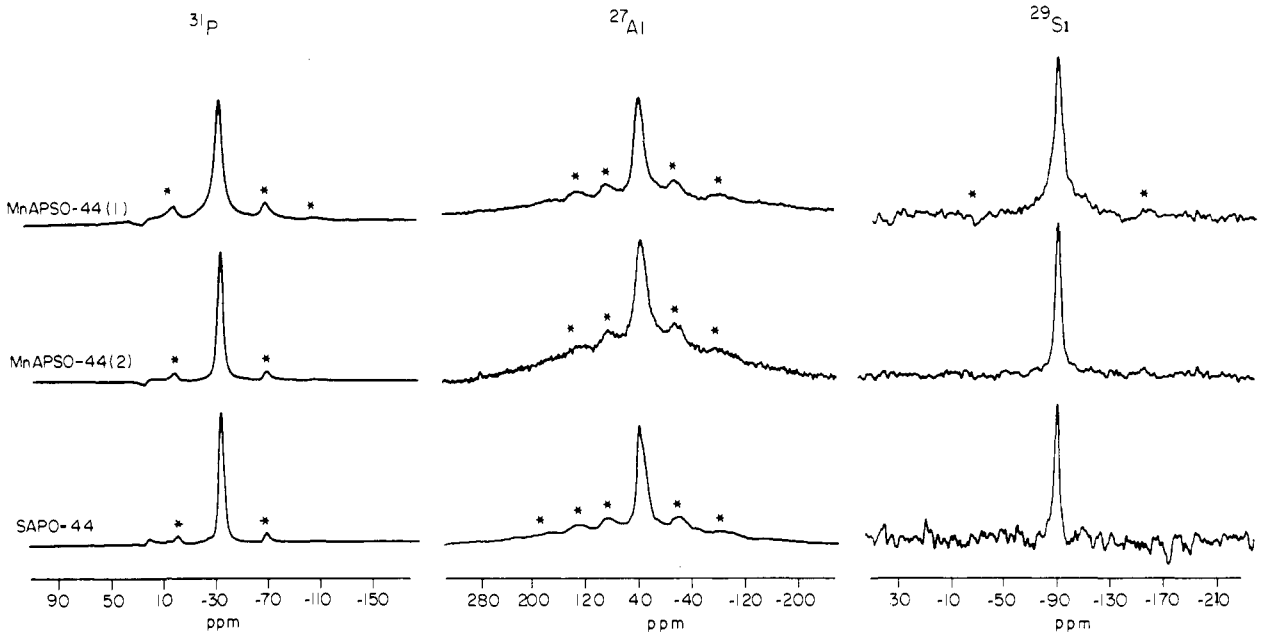

Figure 1. ^{31}P, ^{27}Al, and ^{29}Si MAS NMR spectra of as-synthesized SAPO-44, MnAPSO-44(2), and MnAPSO-44(1). (Asterisks denote spinning sidebands.)

be further interpreted in terms of spatial distribution. Such experiments were found very useful in the case of MnAPO-5.[7]

Experimental Section

Materials. SAPO-44 was synthesized according to procedures described in the literature[2] except that the reaction time was 4 days at 195 °C and the source of Al was pseudo-boehmite. Two MnAPSO-44 samples, termed MnAPSO-44(1) and MnAPSO-44(2), differing in their Mn content were synthesized according to procedures described in ref 13. The composition of the reaction mixture was (1CHA–xMn(OAc)$_2$–0.6SiO_2)–0.9Al_2O_3–0.7P_2O_5–50H_2O (CHA = cyclohexylamine, Ac = acetate ion). For MnAPSO-44(1) x = 0.04 and for MnAPSO-44(2) x = 0.003 and the reaction time was 4 days at 195 °C. The X-ray powder diffraction patterns of the as-synthesized SAPO-44 and MnAPSO-44 materials were similar to those reported in the literature with no evidence of impurities. Scanning electron micrographs show cube-like rhombohedra, the expected morphology of a chabazite-type structure.[14] The compositions of the samples investigated, as obtained from chemical analysis, are given in Table I. The calcination procedure of MnAPSO-44 was as follows: the as-synthesized sample was placed in an already heated oven (500 °C) and calcined under a flow of air (80–100 L/h) for approximately 1 h. After calcination the colorless material became light green-blue, cooling it in a desiccator turned it into light blue-violet, and finally in air it became pale violet-pink. A longer calcination time results in a significant decrease of crystallinity. SAPO-44 was calcined at 550 °C for 2 h. Dehydration was accomplished by heating the sample in vacuum to the desired activation temperature (400 °C) at a rate of 50 °C/h. The samples were left at the dehydration temperature for 2–10 h (at a residual pressure of $\sim 10^{-5}$ Torr) and then sealed under vacuum. The EPR samples were prepared in situ and samples for NMR were kept in sealed tubes until the measurement time. Immediately before the measurements they were transferred, under dry N_2, into tightly sealed rotors.

NMR Measurements. NMR experiments were performed on a Bruker CXP spectrometer operating at 300 MHz for ^1H, 121.44 MHz for ^{31}P, 78.17 MHz for ^{27}Al, and 59.59 MHz for ^{29}Si. The MAS experiments were carried out with a Doty probe. The spinning rate ranged between 3 and 4 kHz and the rotors used were Zirconia with Kel-F caps. A single pulse of 3 μs was applied for ^{31}P and ^{29}Si. Care was taken to apply 15° pulses in the ^{27}Al measurements ($\pi/2$ pulse was 3.8 μs) to ensure that quantitative comparison of signal intensities can be made.

ESR measurements were performed on a Varian E-12 spectrometer, operating at X-band (≈9 GHz) and Q-band (≈35 GHz). The spectra were recorded at low temperature, −80 to −120 °C, and at room temperature (RT). ESEEM measurements were performed at 4 K using a home built spectrometer.[15] The measurements were done using a folded half wave resonator/cavity probehead[16] fitted to a Janis 7.75 DT cryostat. The three-pulse ESEEM ($\pi/2$–τ–$\pi/2$–T–$\pi/2$–τ-echo) experiment was performed with a four-step phase cycle to eliminate unwanted echoes.[17] Typically, the duration of the pulses was 20 ns with a power of about 40 W and the T increment was 20 ns. The ESEEM measurements were recorded at several τ values: 0.2 and 0.22 μs to detect modulation from ^{27}Al nuclei, and 0.26 and 0.28 μs to detect modulation from ^{31}P nuclei.[11]

For the "2 + 1" sequence, θ_0–t–ϕ_0–t_1–θ_0–τ-echo, $t_1 + t = \tau$, the "+1" (middle) pulse was generated by an additional microwave channel with the option of independently changing the amplitude, phase, and length of the pulse. The ratio of H_1^+/H_1 was kept fixed at 3, and the length of the "+1" pulses was 20 or 10 ns. The length of the first and the last pulse was 40 ns. The usual procedure of four-step phase cycling[17] was used to eliminate unwanted ESE signals (stimulated echo and echo induced by the second and third pulses).

Results

NMR Measurements. The ^{29}Si, ^{27}Al, and ^{31}P MAS NMR spectra of as-synthesized SAPO-44, MnAPSO-44(1), and MnAPSO-44(2) are shown in Figure 1. Each spectrum consists of a single resonance at −91, 41, and −28.5 ppm for ^{29}Si, ^{27}Al, and ^{31}P, respectively. The chemical shifts are relative to TMS, a solution of $Al(NO_3)_2$, and phosphoric acid, respectively. This indicates that in SAPO-44 only one type of T atom is present. These values are very similar to those reported for SAPO-34.[18] The absence of a ^{29}Si resonance at ∼−110 ppm indicates that no amorphous silica is present. Furthermore, the presence of only one Si line confirms the chemical analysis results that Si substitutes mostly P and that all Si are surrounded by 4 Al. There is practically no difference between the spectrum of MnAPSO-44(2), where the Mn content is very low, and that of SAPO-44. In contrast, the signals of the ^{31}P and the ^{29}Si of MnAPSO-44(1), where the Mn content is ∼12 times larger than in MnSAPO-44(2), exhibit significant broadening. Furthermore, in the ^{31}P spectrum the intensities of the sidebands are somewhat enhanced due to anisotropic paramagnetic shifts arising from the dipolar interaction of part of the ^{31}P nuclei with the paramagnetic Mn(II).[19] Note that isotropic shifts are not observed in any of the

(13) Lok, B. M. T.; Marcus, B. K.; Flanigen, E. M. *Eur. Pat. Appl.* 0161490A2, 1985.
(14) Dyer, A. *An Introduction to eolite Molecular Sieves*; John Wiley and Sons: Chichester, UK, 1988; p 44.
(15) Goldfarb, D.; Fauth, J.-M.; Tor, Y.; Shanzer, A. *J. Am. Chem. Soc.* **1991**, *113*, 1941.
(16) Britt, R. D.; Klein, M. P. *J. Magn. Reson.* **1987**, *74*, 535.
(17) Fauth, J.-M.; Schweiger, A.; Brauschweiler, L.; Forrer, J.; Ernst, R. R. *J. Magn. Reson.* **1986**, *66*, 74.
(18) Anderson, M. W.; Sulikowski, B.; Barrie, P. J.; Klinowski, J. *J. Chem. Phys.* **1990**, *94*, 2730.

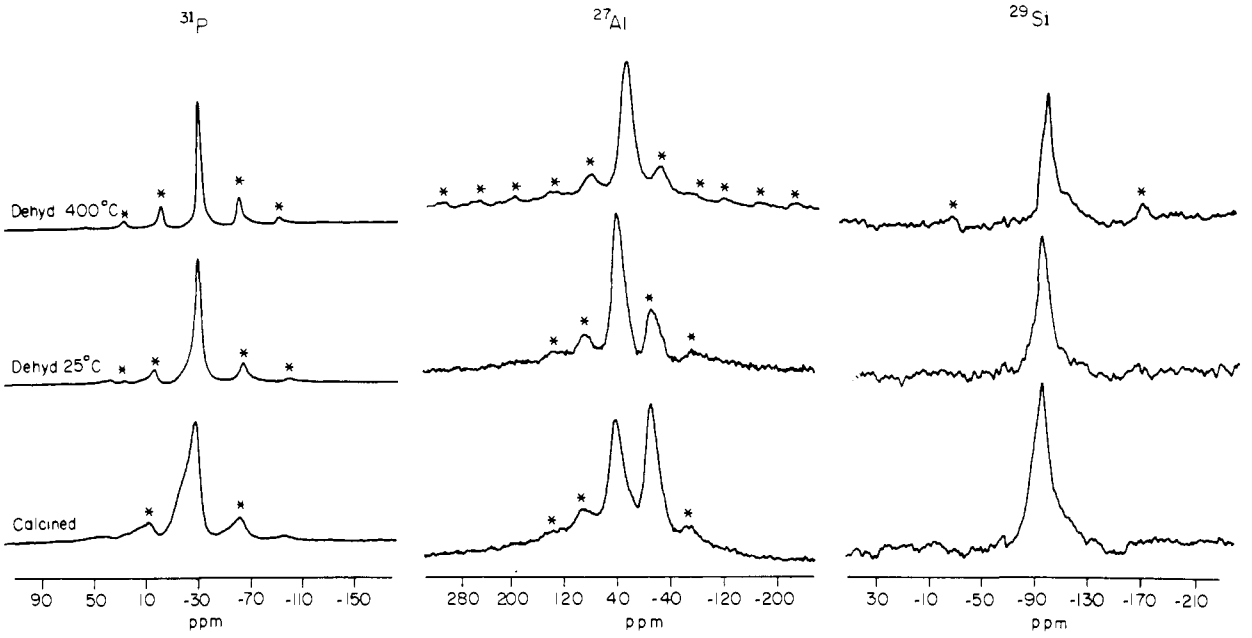

Figure 2. ^{31}P, ^{27}Al, and ^{29}Si MAS NMR spectra of MnAPSO-44(1): calcined, dehydrated at 25 °C, and dehydrated at 400 °C.

spectra of the MnAPSO-44 samples.

Calcination followed by hydration through exposure to air introduced an octahedral Al signal at −13 ppm similar to that observed in other members of the $AlPO_4$ and SAPO families.[18,20] The ^{31}P signal broadened and showed a maximum at −25.5 ppm and a shoulder at a higher field. This behavior is similar to that previously observed in $AlPO_4$-5.[21,22] Similar broadening was observed in the ^{29}Si spectrum. We attribute this broadening to distribution in the chemical shifts induced by water adsorption.[21] Dehydration caused the disappearance of the octahedral Al signal and reduced the width of the ^{31}P and ^{29}Si resonances as expected.[21,22] The same changes were observed in the MnAPSO-44 samples. Figure 2 shows the ^{31}P, ^{27}Al, and ^{29}Si spectra of MnAPSO-44(1) after calcination, dehydration at room temperature, and dehydration at 400 °C. Note that the position of the tetrahedral Al peak changed to −30 ppm upon complete dehydration. This probably reflects changes in the second order quadrupolar shift. The ^{29}Si spectrum shows some sidebands which were not observed in the corresponding SAPO-44 samples, thus we attribute them to interaction with Mn.[19] A close look reveals them also in the spectrum of the as-synthesized sample.

Samples that were calcined and exposed to air for a long time (weeks) and were then dehydrated showed a considerable loss of crystallinity, manifested in a significant broadening of the ^{31}P line. This indicates that the SAPO-44 structure, similar to that of SAPO-37,[23] is not stable when exposed to water vapor in the absence of the template and undergoes hydrolysis which upon dehydration causes structural breakdown. The X-ray pattern of the calcined sample did not show any loss of crystallinity previous to the evacuation, independent of the extent of time to which it was exposed to water vapor. Dehydration of freshly calcined samples did not induce loss of crystallinity.

EPR Measurements. The X-band EPR spectrum of Mn(II) ($S = {}^5/_2$, $I = {}^5/_2$) in a disordered system consists of 6 major lines corresponding to the m_s $|-{}^1/_2\rangle \rightarrow |+{}^1/_2\rangle$ transition split to 6 due to the hyperfine interaction with the Mn nucleus. The other transitions are usually not resolved due to their large anisotropies and they contribute mostly to the background upon which the six narrower lines are superimposed. When the zero field splitting (ZFS) is non-negligible, small peaks in between the 6 major hyperfine lines appear. They represent forbidden transitions involving $\Delta m_I = \pm 1$ and reduce the resolution of the X-band spectrum. These transitions are significantly weaker in the Q-band spectrum since their probabilities are inversely proportional to the external magnetic field;[24] hence, the Q-band spectrum is better resolved. In the following we shall present both X- and Q-band spectra.

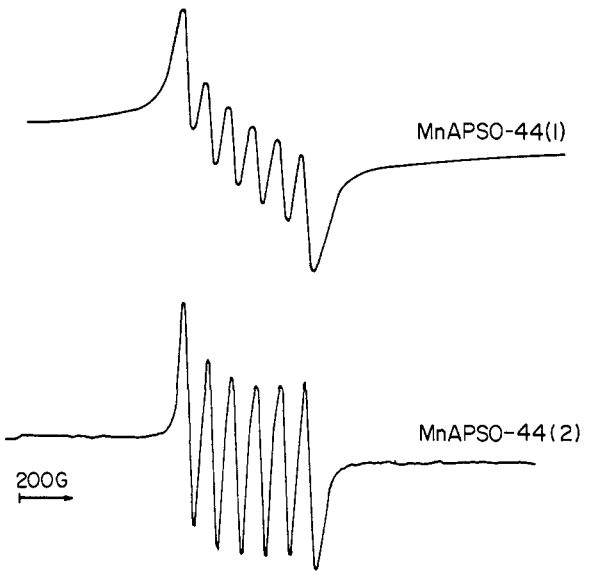

Figure 3. Q-band EPR spectra, recorded at RT, of MnAPSO-44(1) and MnAPSO-44(2).

Figure 3 shows the Q-band EPR spectra of as-synthesized MnAPSO-44(1) and MnAPSO-44(2). The spectrum of MnAPSO-44(2) reveals a single species with $a = 85$ G and $g \simeq 2.00$. The spectrum of MnAPSO-44(1) is very similar; the line width is, however, significantly larger due to the higher Mn(II) content which leads to stronger spin–spin interactions. Due to the lower resolution of the EPR spectrum of MnAPSO-44(1) in the following we shall concentrate mostly on MnAPSO-44(2). Figure 4 shows the X-band EPR spectra of as-synthesized, calcined (hydrated), and dehydrated (400 °C) MnAPSO-44(2) recorded at RT and at low temperatures. Forbidden transitions are evident in all spectra. From spectral simulations we estimate the ZFS parameter, D, to be 140 G in the as-synthesized and calcined

(19) Goldfarb, D. *Zeolites* **1989**, *9*, 509.
(20) Blackwell, C. S.; Patton, R. L. *J. Phys. Chem.* **1984**, *88*, 6135.
(21) Kustanovich, I.; Goldfarb, D. *J. Chem. Phys.* **1991**, *95*, 8818.
(22) Meinhold, R. H.; Tapp, N. J. *J. Chem. Soc., Chem. Commun.* **1990**, 219.
(23) Saldarriaga, L. S.; Saldarriaga, C.; Davis, M. E. *J. Am. Chem. Soc.* **1987**, *109*, 2686.

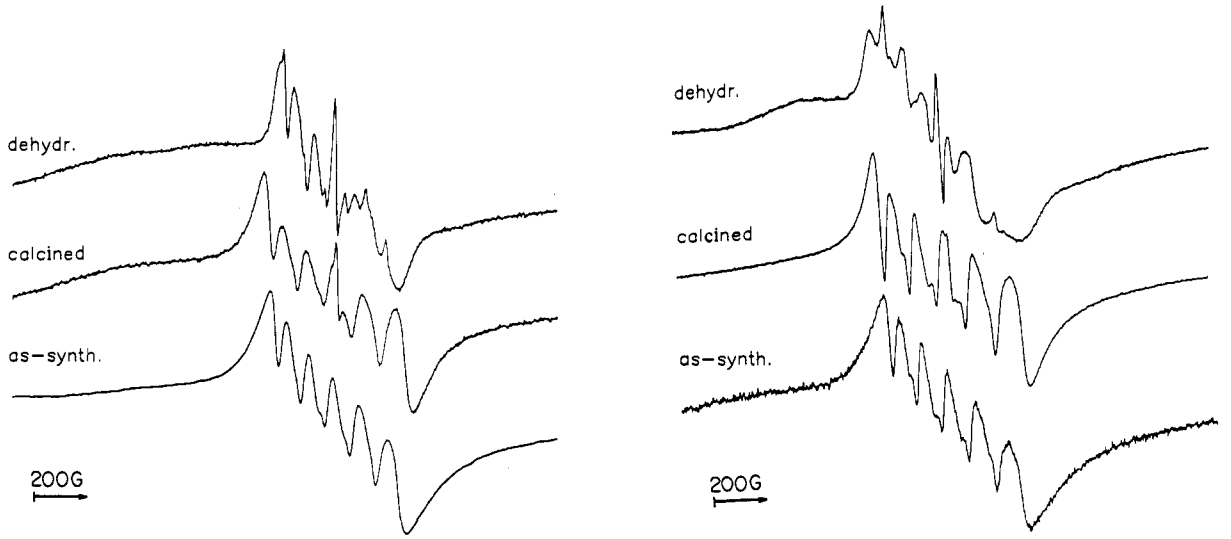

Figure 4. X-band EPR spectra of MnAPSO-44(2): as-synthesized, calcined, and dehydrated at 400 °C recorded at RT (left) and at −130, −90, and −80 °C (right), respectively.

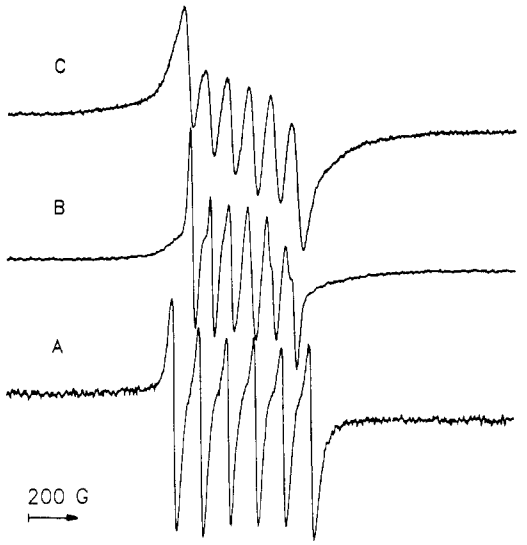

Figure 5. Q-band EPR spectra (recorded at RT): (A) calcined MnAPSO-44(2); (B) dehydrated MnAPSO-44(2); and (C) as in B but after 24 h exposure to air.

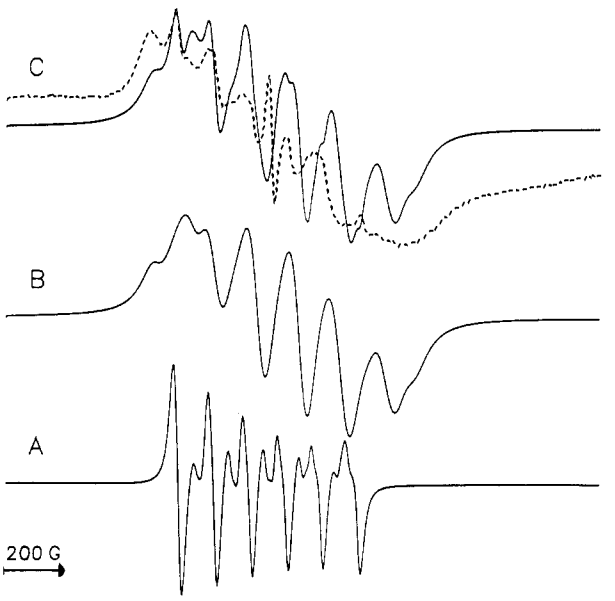

Figure 6. Calculated X-band EPR spectra: (A) a = 65 G, D = 100 G, Δ = 10 G; (B) a = 67 G, D = 260 G, Δ = 30 G; (C) superposition of spectra A and B with ratios of 0.11:1.0, respectively. In both spectra g = 2.01 and the frequency is 9.15 GHz. The dashed trace shows the low temperature X-band spectrum of dehydrated (400 °C) MnAPSO-44(2).

samples.[7,24] Calcination and hydration did not alter the g value but the hyperfine coupling constant, a, increased from 85 to 93 G. The low temperature spectrum of the calcined sample strongly resembles that of a frozen solution of manganese acetate, implying that the Mn(II) is in an octahedral environment very similar to that of $Mn(H_2O)_6^{2+}$. Comparison between the low and room temperature spectra of the calcined sample reveals sharper shoulders in the low temperature spectrum. This suggests that some motion takes place at room temperature. The room temperature Q-band spectrum of calcined MnAPSO-44(2) is shown in Figure 5, trace A. Note that the lines are narrower than in the as-synthesized samples.

While calcination did not produce considerable changes in the EPR spectrum, dehydration at 400 °C did. The total width of the spectrum decreased significantly due to the reduction of a to 65 G as shown by the Q-band spectrum depicted in Figure 5, trace B. The dehydration involves also a color change, from the light pink of the calcined hydrated samples to pale green in the dehydrated state. The corresponding RT and −80 °C X-band spectra are shown in Figure 4. The spectra show an additional sharp line at $g \simeq 2$ which was also observed in the calcined sample. This line is due to some other paramagnetic species, not Mn(II), formed during calcination. Its relative intensity is very low and it will not be discussed any further. The total width of the X-band spectra is reduced as compared to those of the calcined and as-synthesized samples. The spectra portray a mixture of sharp lines separated by 65 G and broader features which suggests the coexistence of two species with significantly different D parameters.

We attempted to reproduce the features of the low temperature spectrum by computer simulations involving a superposition of two spectra. The simulations were done using the expressions given in ref 24 and include only the m_s $|-^1/_2\rangle \rightarrow |^1/_2\rangle$ transitions and the corresponding forbidden transitions. The results are shown in Figure 6. The bottom spectrum corresponds to species A, with parameters a = 65 G, g = 2.01, D = 100 G, and line width (Δ) of 10 G; the middle trace corresponds to species B, with a = 65 G, g = 2.01, D = 260 G, and Δ = 30 G. The top trace shows a superposition of the two with relative intensities (area wise) of A:B = 0.11:1. The calculated spectrum exhibits a qualitative fit in terms of peaks and shoulder positions. There are two main difficulties: one is the presence of the sharp signal in the center of the spectrum that masks one of the hyperfine line; the second is the broad background which is present in the experimental

(24) Meirovitch, E.; Poupko, R. *J. Phys. Chem.* **1978**, *82*, 1920.

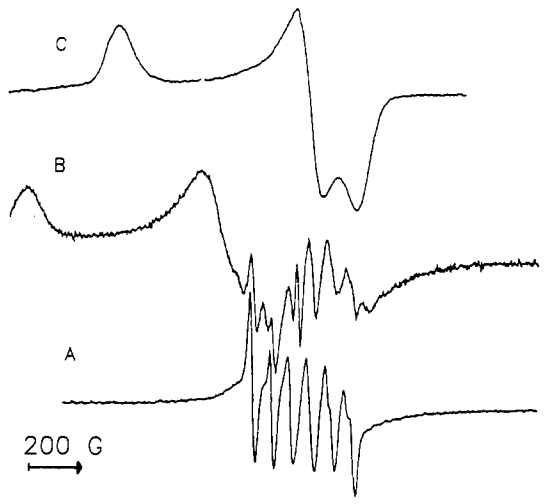

Figure 7. Q-band EPR spectra (recorded at RT): (A) dehydrated (400 °C) MnAPSO-44(2); (B) same as A, but for a sample with partial structural breakdown; (C) X-band spectrum (RT) of a MnAPSO-44(2) sample dehydrated (400 °C) with complete loss of crystallinity.

spectrum and affects the relative intensities of the various peaks. This background is absent in the calculated spectra since only the $|-^1/_2\rangle \rightarrow |^1/_2\rangle$ transitions were considered. Any attempts to reproduce the spectrum using one species failed. The main difficulty was to simulate the sharp features. Introducing an $E \neq 0$, namely a non-axial zero field tensor, did not produce the sharp features. Within a series of dehydrated samples the relative intensities of the sharp peaks varied supporting the existence of two Mn(II) species. The RT spectrum of MnAPSO-44(2) dehydrated at 400 °C differs significantly from the low temperature spectrum (Figure 4). While the "narrow lines" appear at the same positions, the total width of the spectrum is substantially decreased. This suggests the existence of some motion in species b that partially averages the anisotropy caused by the ZFS. The spectral features of the Q-band spectrum recorded at room temperature could not be reproduced by a static spectrum of a single species.

After the EPR measurement of the dehydrated sample the EPR tube (Q-band capillary) was broken at the top and left exposed to air. The water adsorption in this case was very slow. After 48 h two phases were evident in the tube, the top phase was pink, a characteristic color of octahedral Mn(II)[25] and indicative of water coordination, and the bottom remained greenish. The Q-band spectrum, depicted in Figure 5C, shows splitting of 75 G which is in between that of the calcined hydrated and the dehydrated sample. After a week the whole sample turned pink and the original spectrum of the calcined sample was regenerated. X-ray diffraction collected after the sample was opened indicated that the sample kept its crystallinity, although some minor broadening was observed.

It was mentioned earlier that calcined hydrated samples which were left to stand for a long time lost their crystallinity upon dehydration. The Mn(II) EPR spectrum was found to be particularly sensitive to this structural breakdown. Figure 7 shows the spectra of samples of MnAPSO-44(2) which underwent such a breakdown. The middle trace spectrum is of a freshly dehydrated sample and consists of a superposition of two types of signals. One is that observed in dehydrated MnAPSO-44(2) (compare with bottom spectrum) along with additional new features, probably corresponding to the six lines of another Mn(II) species. The other signal is broad and shows a peak at $g = 2.43$. A few days later, the six-line patterns disappeared completely and the spectrum observed is characteristic of a non-axial g tensor with $g_x = 1.9$, $g_y = 2.0$, and $g_z = 2.43$. Comparison between X- and Q-band spectra confirmed the assignment. This spectrum is very unusual for Mn(II). It shows no hyperfine splitting which is characteristic of a strong Heisenberg exchange between the Mn species and a large g anisotropy. The latter is very unusual for a d^5 high spin configuration, hence this spectrum cannot be of an isolated Mn(II) species. The lack of hyperfine splitting may suggest the formation of a unique Mn clusters with an effective $S = {}^1/_2$. The formation of Mn(III) or Mn(IV) can be excluded since the EPR spectrum can be observed at room temperature. The X-ray diffraction pattern of this sample showed complete loss of crystallinity. Since this signal is typical for a sample that has lost its structure we did not investigate it any further. A sample that was dehydrated close to the calcination and was kept in a sealed tube showed no signs of decomposition also after 6 months.

ESEEM Measurements. ESEEM measurements were carried out to probe the close environment of the Mn(II) in as-synthesized, calcined (hydrated), and dehydrated samples. Figure 8 shows the three-pulse ESEEM recorded at $\tau = 0.26$ μs at which the ^{31}P modulation depth is maximized and the Al modulation is suppressed.[11] The ESEEM were recorded at 3155 G, close to the center of the spectrum. The Fourier transforms (FT) of the time domain traces are shown in Figure 8 as well. Prior to the FT the background decay was removed and the data were convoluted with a Hanning window. A peak at 5.4 MHz, which is the ^{31}P Larmor frequency, is evident in all spectra. A strong peak at 13.5 MHz corresponding to protons appears in the as-synthesized and calcined samples. The relative intensities of the various peaks are proportional to the modulation depth. The modulation depth of the ^{31}P in the calcined samples and that in the dehydrated samples are similar, suggesting that the position of the Mn(II) with respect to the ^{31}P nuclei has not changed as a consequence of dehydration. The ^{31}P peak in the as-synthesized sample is somewhat weaker. Note that the dehydrated sample still shows a weak peak of protons. All samples revealed no splitting of the Larmor frequency, hence the isotropic hyperfine constant of the ^{31}P is $\simeq 0$.

The ESEEM time domain traces recorded at $\tau = 0.20$ μs ($H = 3155$ G) along with the corresponding FT-ESEEM spectra are shown in Figure 9. For this particular τ the proton peak is suppressed and the spectra are dominated by the ^{27}Al peak at 3.5 MHz. While both the as-synthesized and the calcined samples show an ^{27}Al peak with comparable intensities the dehydrated sample shows practically no modulation. Since no significant changes were observed in the ^{31}P modulation due to the dehydration process we attribute this decrease to a significant increase in the quadrupole interaction of the Al nuclei.[26,27] This increase in the quadrupole coupling constant is not general for all Al in the sample since the ^{27}Al MAS NMR spectra of dehydrated samples of MnAPSO-44 did not show any significant broadening although it did show a change in peak position. Accordingly, we deduce that the large increase in the quadrupole coupling constant is only for those Al in the close vicinity of the Mn(II) and the distortion of their tetrahedra is a consequence of their proximity to the Mn(II). Due to the very low content of the Mn(II) only a few Al sites are affected, not enough to be evident in the NMR spectrum which represents all Al in the sample. Interestingly, we also obtained a weak echo from MnAPSO-44(1) which showed very weak Al modulation under the same experimental conditions.

"2 + 1" ESE Results. "2 + 1" ESE experiments were performed on as-synthesized and calcined MnAPSO-44(2). The pulse sequence employed was θ_0–t–ϕ_0–t_1–θ_0–τ-echo, where θ_0 is the nominal flip angle of the first and the last pulse, namely $\theta_0 = \gamma H_1 t_p$ where t_p is the pulse length. ϕ_0 is the nominal flip angle of the "+1" pulse ($\phi_0 = \gamma H_1{}^+ t_p{}^+$) and $t + t_1 = \tau$. In this experiment τ is held constant and the echo intensity is measured as a function of t.[12] The optimized experimental conditions, namely the lengths and amplitudes of the pulses, were similar to those used in our previous study,[7] $H_1{}^+/H_1 = 3$ and $t_p/t_p{}^+ = 2$, yielding $\phi_0/\theta_0 = 3/2$, excluding one measurement where $t_p/t_p{}^+ = 4$ ($\phi_0/\theta_0 = 3/4$). Several measurements at different ϕ_0 values, in the range $(0.4–0.7)\pi$, were performed for each sample. Typical results for $\phi_0 = 0.58\pi$ and 0.59π for the calcined and as-synthesized sample,

(25) Cotton, F. A.; Wilkinson, G. *Advanced Inorganic Chemistry*; Wiley Eastern Private Limited: New Delhi, 1966; Chapter 29.

(26) Goldfarb, D.; Kevan, L. *J. Magn. Reson.* **1989**, *82*, 270.
(27) Matar, K.; Goldfarb, D. *J. Chem. Phys.* **1992**, *96*, 6464.

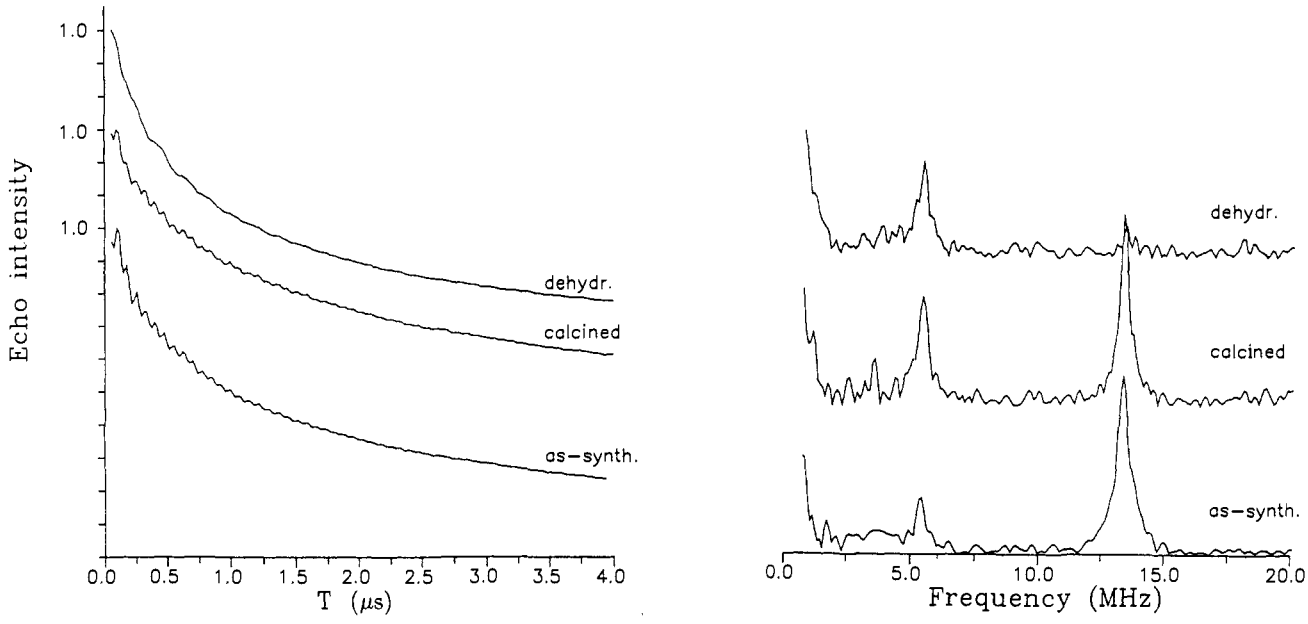

Figure 8. Three-pulse ESEEM of MnAPSO-44(2), τ = 0.26 μs, H = 3155 G: (left) time domain, (right) the corresponding magnitude FT-ESEEM spectra.

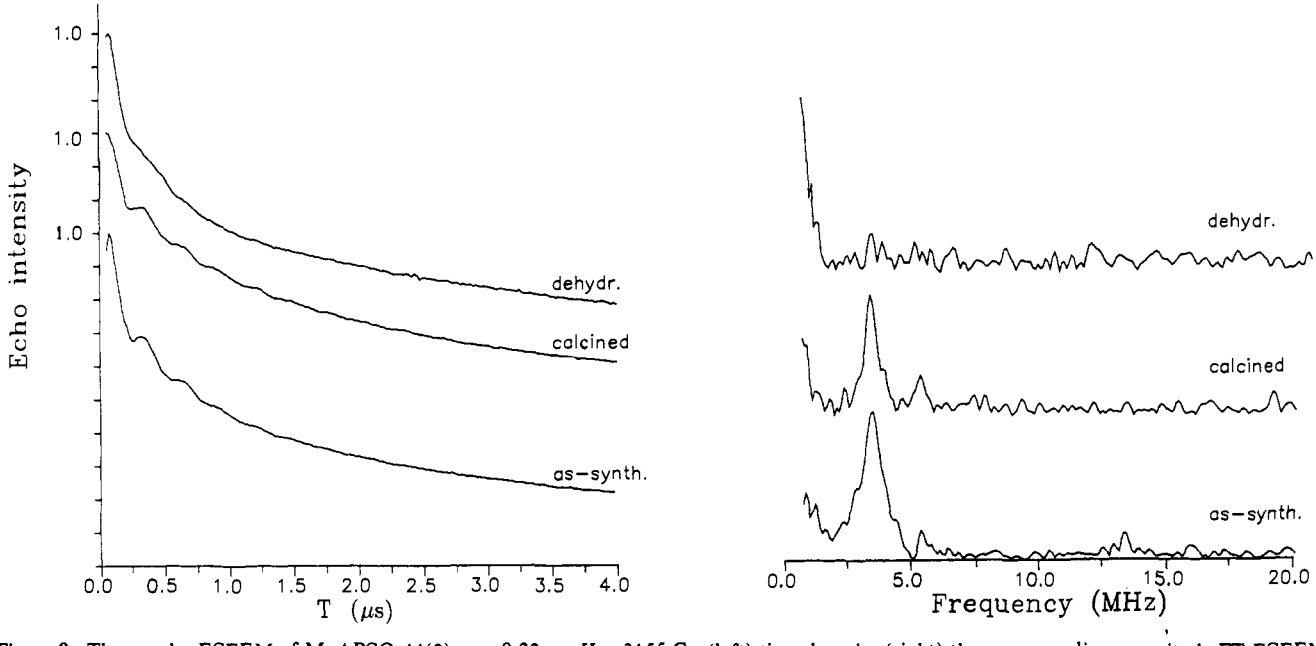

Figure 9. Three-pulse ESEEM of MnAPSO-44(2), τ = 0.22 μs, H = 3155 G: (left) time domain, (right) the corresponding magnitude FT-ESEEM spectra.

respectively, are shown in Figure 10. The flip angle ϕ_0 was determined from V_0^+/V_0 which is the ratio of the echo intensity with the "+1" pulse and without it.[7,12]

The general expressions for the "2 + 1" echo intensity were developed for the case of $S = {}^1/_2$.[12] Here we apply this experiment to a $S = {}^5/_2$ system with a significant ZFS. Hence, it is reasonable to assume that only part of the $m_s\ |-{}^1/_2\rangle \rightarrow |{}^1/_2\rangle$ transitions are excited by the microwave pulse. In this case the nutation frequency is not γH_1 but $\gamma(3H_1)$.[28-30] Accordingly, the H_1 and H_1^+ referred to in the definition of the nominal flip angles θ_0 and ϕ_0 correspond to the effective H_1 and H_1^+ which are really $3H_1$ and $3H_1^+$. Furthermore, the expressions for V_0^+/V_0 and for $\langle SC\rangle$[12] apply as well, noting again that γH_1 and γH_1^+ refer to effective nutation frequencies.

In the case of randomly distributed paramagnetic centers the echo decay is given by[12]

$$\ln V^+(t) = -2kCt\langle SC\rangle \qquad (1)$$

where C is the spin concentration and k for Mn(II) ($S = {}^5/_2$) is 2.77×10^{-12} cm^{-3} s^{-1}. $\langle SC\rangle$ is given by[7]

$$\langle SC\rangle = \langle \sin^2(\phi/2)\cos\theta\rangle_{g(\omega)} = \int_{-\infty}^{\infty}\left[\frac{(\gamma H_1^+)^2}{\Delta\omega^2 + (\gamma H_1^+)^2}\sin^2\left(0.5\phi_0\left(1 + \frac{\Delta\omega^2}{(\gamma H_1^+)^2}\right)^{1/2}\right)\right] \times \left[1 - 2\frac{(\gamma H_1)^2}{\Delta\omega^2 + (\gamma H_1)^2}\sin^2\left(0.5\theta_0\left(1 + \frac{\Delta\omega^2}{(\gamma H_1)^2}\right)^{1/2}\right)\right] g(\omega)\, d\omega \qquad (2)$$

where $\langle\cdots\rangle_{g(\omega)}$ means averaging over the whole EPR line shape to include all off-resonance effects and $\Delta\omega = \omega_0 - \omega$ where ω_0 is

(28) Samoson, A.; Lippmaa, E. *J. Magn. Reson.* **1988**, *79*, 255.
(29) Kentgens, A. P. M.; Lemmens, J. J. M.; Geurtz, F. M. M.; Veeman, W. S. *J. Magn. Reson.* **1987**, *71*, 62.
(30) Isoya, J.; Kanda, H.; Noris, J. R.; Tang, J.; Bowman, M. K. *Phys. Rev. B* **1990**, *41*, 3905.

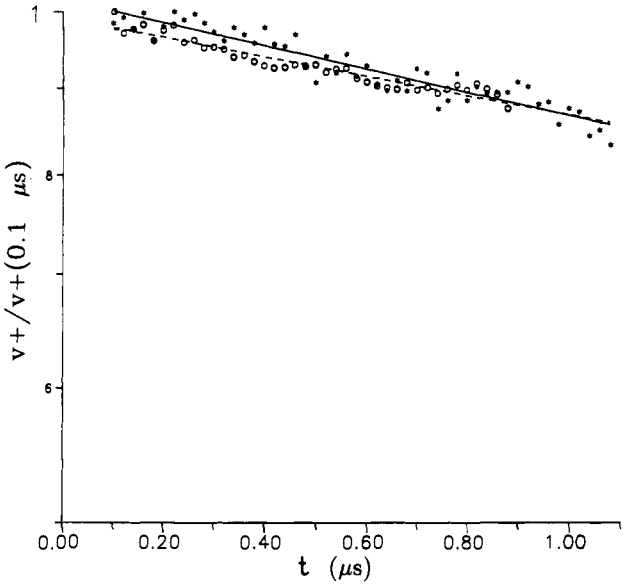

Figure 10. Plot showing the "2 + 1" spin echo decays of as-synthesized (O) and calcined (•) MnAPSO-44(2) recorded at (SC) = 1.8×10^{-2} and 1.7×10^{-2}, respectively. The solid and dashed lines give the best exponential fit.

the carrier frequency of the microwave pulses. When integration over the whole EPR line shape is performed, contributions from transitions other than the m_s $|-1/2\rangle \rightarrow |1/2\rangle$ transitions are also taken into account, because these transitions produce the broad background of the EPR spectrum. But since these were not taken into account in the expressions for ⟨SC⟩ and for the echo intensity[12] this may lead to inaccuracies. However, based on the control experiments previously performed we conclude that the inaccuracies are within the experimental error.[7] In the control experiments the " 2 + 1" method was applied to frozen solutions of Mn^{2+} in water/glycerol with known concentrations. The good agreement between the obtained results and the known concentrations indicates that our assumptions are reasonable.

Using eq 2 we calculated ⟨SC⟩ for the various experiments differing in ϕ_0 and θ_0. Figure 11 shows the dependence of the echo decay rate, $2kC\langle SC\rangle$, on ⟨SC⟩ for the two samples studied. From the slopes we determined the spin concentration of the homogeneously distributed Mn(II) species. For the as-synthesized sample we obtained $1.5 \pm 0.2 \times 10^{18}$ spins cm^{-3} and for the calcined sample $1.69 \pm 0.2 \times 10^{18}$ spins cm^{-3}. The difference between the two samples is practically insignificant, thus we conclude that no change in the spatial distribution has occurred in the sample with respect to the homogeneously distributed spins due to calcination. This should be compared to the Mn content as obtained from chemical analysis. The X-ray structure of SAPO-44 has not been determined but is known to be close to that of SAPO-34 which has a chabazite-like structure.[31,32] The volume of a unit cell of chabazite is 822 Å.[33] Assuming that the unit cell volume of MnAPSO-44 is similar and that a unit cell contains a total of 12 T atoms and that all the Mn(II) remains as Mn(II), we obtained a spin concentration of 10×10^{18} spins/cm^{-3} for a Mn content of 0.07 atom %. This is more than 5 times the value obtained from the "2 + 1" ESE experiment, indicating that not all Mn in the sample contribute to the echo.

Discussion

In this work we concentrated mostly on the investigation of the close environment of Mn(II) in MnAPSO-44(2) in various states, namely as-synthesized, calcined (hydrated), and dehydrated. A

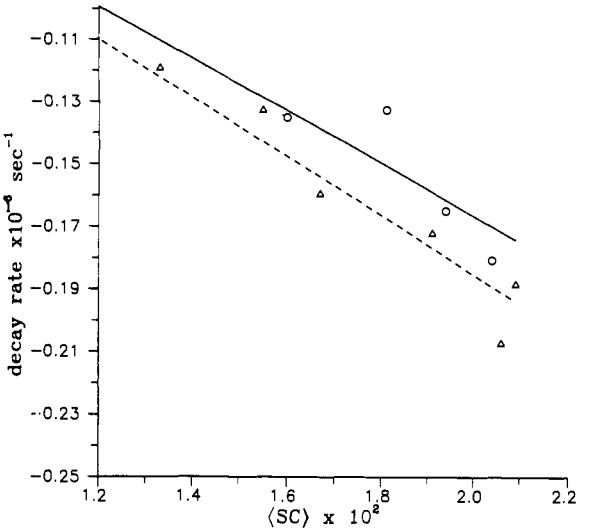

Figure 11. Plot showing the dependence of the echo decay rates of as-synthesized (Δ) and calcined (O) MnAPSO-44(2) on ⟨SC⟩.

difficulty we encountered was the instability of calcined SAPO-44 toward dehydration once the calcined sample was exposed to water vapor for long periods. This has been observed for both SAPO-44 and MnAPSO-44, and for the latter the EPR spectrum of the Mn(II) was found to be extremely sensitive to structural breakdown. It has been recently reported that SAPO-34 also undergoes some structural breakdown after calcination, exposure to water vapor, and dehydration.[34] Other members of the family such as SAPO-5[35] and SAPO-11[9] are stable in the calcined state whereas SAPO-37[23,35] is not. There is, however, a significant difference between the stability of calcined SAPO-37 and SAPO-44. While calcined SAPO-37 decomposed at room temperature upon exposure to water vapor, SAPO-44 showed signs of decomposition only after dehydration was attempted. Nonetheless, SAPO-44 maintained its crystallinity once the dehydration was performed close to the calcination. The similarity between SAPO-44, SAPO-34, and SAPO-37 as opposed to SAPO-5 and SAPO-11 may lie in their different Si, Al, and P ordering in the framework. In SAPO-37 and SAPO-44 Si seems to replace mostly P whereas in the SAPO-5 and SAPO-11 it substitutes for both P and Al.[18,35] This should result, for the former two, in a sample with more Brønsted acid sites which may contribute to their instability. Indeed higher acidity has been reported recently for SAPO-34 and SAPO-37 as compared to SAPO-5.[36] Another possibility is that SAPO-44, SAPO-34, and SAPO-37 are related to aluminosilicate structures (chabazite and faujasite) and their different compositions may lead to slightly different bond lengths and angles rendering the structure less stable. The NMR results confirmed that the Si substitutes mostly for P since only one peak for both Si and P is observed. Both the NMR and the ESEEM spectra showed no isotropic hyperfine coupling between the Mn(II) and framework nuclei. Such an interaction in the as-synthesized material would have provided direct evidence for framework substitution.

The EPR spectrum of as-synthesized MnAPSO-44(2) shows a hyperfine splitting of 85G and is very similar to that of as-synthesized MnAPO-5,[7] MnAPO-11,[8] and MnAPSO-11[9] with comparable Mn content. In MnAPO-5 the Mn was found to be in extraframework sites whereas in MnAPO-11 and MnAPSO-11 it was reported to be incorporated into the framework. Accordingly, in this case the EPR spectrum of the as-synthesized sample alone cannot provide any indication for framework substitution.

(31) Ito, M.; Shimoyama, Y.; Saito, Y.; Tsurita, Y.; Otake, M. *Acta Crystallogr.* **1985**, *C41*, 1698.
(32) Bennett, J. M.; Marcus, B. K. *Innovation in Zeolite Materials Science*; Grobet, P. J., et al., Eds.; Elsevier: Amsterdam, 1988; p 264.
(33) Breck, D. W. *Zeolite Molecular Sieves*; Robert E. Krieger Pub. Co.: Malabar, FL, 1984.
(34) Vomscheid, R.; Briend, M.; Souron, J. P.; Barthomeuf, D. Extended Abstract, Ninth International Zeolite Conference, Montreal, July 1992.
(35) Briend, M.; Shikholeslami, A.; Peltre, M. J.; Delafosse, D.; Barthomeuf, D. *J. Chem. Soc., Dalton Trans.* **1989**, 1361.
(36) Minchev, Chr.; Neinska, Ya.; Valtchev, V.; Minkov, T.; Tsoncheva, T.; Penchev, V.; Lechert, H.; Hess, M. Extended Abstract, Ninth International Zeolite Conference, Montreal, July 1992.

Calcination caused an increase in a to 93 G and the spectrum resembles very much to that of $Mn(H_2O)_6^{2+}$. Thus, in the calcined samples the Mn(II) is in an octahedral symmetry. This is also supported by the pinkish color.[25] The difference between the room temperature and low temperature spectra indicates some motional effects which can be attributed to exchange of water ligands. The octahedral symmetry in hydrated samples does not necessarily contradict framework substitution. In calcined hydrated AlPOs and SAPOs a significant part of the framework Al assumes an octahedral symmetry by coordinating two water molecules.[18,20-22] Octahedral Al peaks were observed in the ^{27}Al MAS NMR spectra of hydrated SAPO-44 and MnAPSO-44. Accordingly, it is possible that also Mn(II), if situated in the framework, could coordinate two water molecules and obtain an octahedral symmetry. Dehydration caused a significant decrease in a, from 93 G to 65 G. Such a low hyperfine constant can be explained either by a significant increase in the covalency of the bonding[37] or alternatively by a change from octahedral to tetrahedral coordination.[38] We find the second possibility more plausible since the nature of the ligands available for the Mn(II) in the dehydrated state (framework oxygen and/or OH) is not that different from those available in the hydrated case such as to induce a change of ~25 G in the Mn(II) hyperfine constant. Accordingly, we find the EPR results consistent with a model where most of the Mn(II) ions are located in framework sites. In the calcined hydrated state they are bound to four framework oxygens and to two water molecules. Removal of the water leaves tetrahedral Mn(II) coordinated to framework oxygen only. This is consistent also with the invariance of the ^{31}P modulation depth toward dehydration and the resumed octahedral symmetry after rehydration. It is not clear, however, why the ^{31}P modulation depth slightly increased upon calcination. In MnAPO-5, dehydration of samples with similar Mn content showed significant spin exchange[7] indicating Mn(II) migration, and in MnAPO-11 dehydration reduced a only to 87 G.[8] We note, however, that the results do not unambiguously rule out a model where the Mn(II) is non-framework. In this case the Mn(II) in the hydrated samples may be coordinated to three framework oxygens and three water molecules. Dehydration would remove the water molecules leaving one OH ligand to account for the tetrahedral symmetry and the unchanged ^{31}P modulation depth. (The origin of the OH is nonetheless hard to explain.)

The coexistence of two species with different ZFS parameters, D, in the dehydrated samples may be interpreted in terms of different numbers of P and Si neighbors. For instance a Mn(II) in a site surrounded by four P is expected to be less distorted than in a site with 3 P and 1 Si neighbors. The probability of the first is smaller and indeed only ~10% of the signal is attributed to the species with a low D. In the calcined samples both these Mn(II) sites are distorted by water coordination hence exhibiting similar spectra. This rather simple picture fails, however, to explain the motional effects observed in only one of the species. If the Mn(II) is coordinated only to four framework oxygens in the dehydrated state then it cannot be involved in any motion. Another possible explanation can be that the large D arises from a nearby OH group, i.e. one of the neighboring oxygens of the Mn(II) is part of a bridging (or terminal) OH group, which distorts the MnO_4 tetrahedra. Such bridging OH groups were found in NiAPSO-34 where extended X-ray absorption fine structure (EXAFS) was employed to prove that the Ni occupies framework sites.[39] These serve to compensate the negative charge of the framework in the dehydrated state. In the as-synthesized material the charge is compensated by the protonated template. Some mobility of the proton on the bridging OH group or some motion of the whole OH group will result in the dynamics observed. The presence of a nearby proton is supported by the weak proton signal observed in the ESEEM spectrum of the dehydrated sample (Figure 8).

In the absence of motion and neglecting line width effects, the width, δ, of the powder spectrum of a single hyperfine line corresponding to m_I is[40]

$$\delta = \frac{50}{9}\frac{D^2}{H_0} - \frac{2750 m_I a D^2}{81 H_0^2} \qquad (3)$$

Thus, for D = 250 G and neglecting the second term in eq 3, δ is 107 and 27 G for X- and Q-band, respectively. In order to see some narrowing in the X-band spectrum the correlation time of the motion, $1/\tau$, should be on the order of 10^8 s^{-1}. An intermediate rate for the X-band frequency may already be in the fast range for the Q-band frequency. The estimated rate of 10^8 s^{-1} corresponds only to those OH groups in the vicinity of the Mn(II) and cannot be generalized to all acid sites in the sample. Whether it involves only jumps of the proton in case of a bridging hydroxyl or a motion of the OH group in the case of a terminal group cannot be judged from our experimental results, although a proton jump is expected to average the ZFS more effectively than local librations of a terminal OH.

NMR studies on dehydrated H- and D-rho zeolites showed that the majority of the protons/deuterons are rather immobile, namely $1/\tau < 10^4$ s^{-1}.[41] Nonetheless, for the case of D-rho about 7% of the deuterons were found to be highly mobile, namely completely averaging their quadrupole interaction, for those $1/\tau > 10^7$ s^{-1}. The authors suggested that the mobile deuterons correspond to terminal OH groups. On the basis of the above, it is tempting to assign the motion to a terminal OH rather than to migration/diffusion of the proton. Whether this comparison is legitimate is still questionable since the mobility of a proton in the environment of an AlO_4^- and $M_nO_4^{2-}$ may be significantly different due to the different charges. To conclude, we extend our model to include two species of framework Mn(II) in the dehydrated sample, one without a neighboring OH group and with a small D and the second with a bridging OH group and hence a larger D.

The ^{31}P modulation depth can in principle be analyzed in terms of number and distances of ^{31}P nuclei from the Mn(II) center. In our study of MnAPO-5[7] we showed that the modulation depth was lower than expected if Mn were in the framework. However, in these calculations we treated the Mn(II) as a pseudo $S = {}^1/_2$ system and did not consider the effect of the ZFS on the modulation depth. It has been recently suggested that this should be taken into account[42] thus the analysis is not straightforward. Moreover, unlike in the case of MnAPO-5 in MnAPSO-44 the Si, P, and Al distribution should be considered to estimate the number of P neighbors. Nonetheless, as mentioned previously, the P modulation results support the immobility of the Mn with respect to dehydration.

The "2 + 1" ESE experiments indicated that only 15% of the Mn ions are homogeneously distributed and contribute to the echo signal in both the as-synthesized and calcined MnAPSO-44(2) samples. An inhomogeneous distribution of Mn(II) which includes Mn(II) "rich" areas where the spin–spin interactions are strong enough to cause short phase memory time will result in the above situation. Another possibility is the presence of Mn in oxidation states other than +2 which do not contribute to the echo signal even at 4 K due to very short relaxation time. The latter possibility seems less plausible since it is unlikely that Mn(III) or Mn(IV) will be formed during the synthesis and be present in the as-synthesized sample. The amount of homogeneously distributed spins in MnAPSO-44(2) is rather close to that observed in MnAPO-5[7] with similar Mn content. In the latter, migration of the Mn in the areas richer in Mn was evident whereas in MnAPSO-44(2) it was not. The question that arises is whether a homogeneous distribution, as in frozen solutions of Mn(II),[7] is to be expected at all. The answer to the above requires the extension of such studies to more materials of this type.

(37) Lifshitz, E.; Francis, A. H. *J. Phys. Chem.* **1982**, *86*, 4714.
(38) Levanon, H.; Luz, Z. *J. Chem. Phys.* **1968**, *49*, 2031.
(39) Thomas, J. M.; Xu, Y.; Catlow, C. R. A.; Couves, J. W. *Chem. Mater.* **1991**, *3*, 667.
(40) Meirovitch, E.; Luz, Z.; Kalb (Gilboa), A. J. *J. Am. Chem. Soc.* **1974**, *96*, 7542.
(41) Vega, A. J.; Luz, Z. *J. Phys. Chem.* **1987**, *91*, 365.
(42) Coffino, A. R.; Peisach, J. *J. Chem. Phys.* **1992**, *97*, 3072.

Conclusions

Only one type of TO_4 site was found in SAPO-44 and MnAPSO-44. The Si substitutes mostly for P and in hydrated samples part of the Al assumes octahedral coordination. The highly crystalline structures of SAPO-44 and MnAPSO-44 break down upon dehydration of calcined samples which underwent prolonged exposure to water vapor.

Mn(II) in MnAPSO-44 with low Mn content (0.07 atom %) assumes octahedral coordination in the calcined hydrated samples. Dehydration to 400 °C changes the Mn(II) coordination to tetrahedral as evident by the considerable decrease in the hyperfine coupling constant from ~90 to 65 G. These results are consistent with Mn(II) situated in the framework. In the hydrated sample the Mn(II) is coordinated to four framework oxygens and two water molecules whereas in the dehydrated sample it is coordinated only to four framework oxygens one of which is part of an OH group. The Mn(II) framework substitution for Al is supported by relatively weak ^{27}Al modulation and ^{31}P modulation rather invariant to calcination and hydration.

The distribution of the Mn(II) throughout the sample in both as-synthesized and calcined samples in MnAPSO-44 (0.07 atom %) was found to be inhomogeneous. Only about 15% of the Mn(II) is distributed homogeneously and the rest is situated in areas "rich" in Mn(II).

Acknowledgment. This study was supported by funds granted to D.G. through a fellowship program sponsored by the Charles H. Revson Foundation. J.B. gratefully acknowledges the financial support from the National Slovene Board for Science and Technology (RSRDT), Grant No. C2-0538-104. We thank Professor L. Kevan for making refs 8 and 9 available to us prior to publication.

A Novel Approach for Stereochemical Analysis of 1-Carboxyethyl Sugar Ethers by NMR Spectroscopy†

Wayne B. Severn‡ and James C. Richards*

Contribution from the Institute for Biological Sciences, National Research Council of Canada, Ottawa, Ontario, Canada K1A OR6. *Received July 3, 1992*

Abstract: A general strategy for the stereochemical analysis of 1-carboxyethyl sugar ethers is introduced in which the chirality of the lactyl group is related to that of the sugar moiety in a conformationally rigid lactone derivative. With the aid of molecular modeling, the stereochemistry is determined through the use of NOE measurements. This procedure was evaluated using synthetic diastereomeric samples of (*R*)- and (*S*)-methyl 3-*O*-(1-carboxyethyl)-α-L-rhamnopyranoside, and it was successfully applied to the stereochemical analysis of *N*-acetylmuramic acid. The generality of this approach is illustrated here with a 4-O-substituted 1-carboxyethyl sugar ether. It was found that the lactyl group of 4-*O*-(1-carboxyethyl)-D-mannopyranose, which was obtained from the capsular polysaccharide of *Rhodococcus equi* serotype 3, has the (*S*)-configuration.

Introduction

Bacterial cell surface polysaccharides frequently carry acidic non-carbohydrate components, which have been shown to be dominant antigenic determinants contributing to the polysaccharides' serological specificities.[1] Pyruvic acid, linked to a sugar residue as a cyclic acetal, is among the most frequently encountered acidic substituents.[1a,b]

Although less commonly encountered than pyruvic acid acetals, lactic acid ethers, which share a common biosynthetic precursor, are found as substituents (1-carboxyethyl) of a wide range of sugars.[1c] The 3-O-substituted (*R*)-1-carboxyethyl derivative of 2-amino-2-deoxy-D-glucose (muramic acid) and the related manno isomer are components of bacterial cell wall peptidoglycan.[2,3] Lactic acid ether-substituted sugars are also components of bacterial cell wall lipopolysaccharides and of extracellular polysaccharides. Both the (*R*)- and (*S*)-enantiomers of the lactyl group have been reported as substituents of D-glucose (substituted at the 4-position)[4-9] and L-rhamnose (substituted at the 3-position),[10-13] whereas only the (*S*)-enantiomer has been found as a substituent (at the 4-position) of D-mannose[14-16] and D-glucuronic acid.[17,18] Lactic acid ethers have also been found linked to the O-4 positions of D-galactose[19] and L-rhamnose,[20] although their chiralities have not been determined.

The structural diversity of these antigenic determinants is influenced by (i) the nature and configuration of the substituted monosaccharide residue, (ii) the position of the hydroxyl group that is substituted, and (iii) the chirality of the substituent.

The stereochemistry of the substituted monosaccharide can be readily determined after removal of the lactic acid moiety.

† Issued as National Research Council of Canada publication No. 34281.
‡ NRCC Research Associate 1988-1990.

(1) (a) Kenne, L.; Lindberg, B., In *The Polysaccharides*; Aspinall, G. O. Ed.; Academic Press Inc.: New York, **1983**, *2*, 287. (b) Heidelberger, M.; Dudman, W. F.; Nimmich, W. *J. Immunol.* **1970**, *104*, 1321. (c) Lindberg, B. *Adv. Carbohydr. Chem. Biochem.* **1990**, *48*, 279. (d) Jennings, H. J. *Adv. Carbohydr. Chem. Biochem.* **1983**, *41*, 155. (e) Lee, C.-J. *Mol. Immunol.* **1987**, *24*, 1005. (f) Schiffman, G., *Rev. Infect. Dis.* **1981**, *3* (Suppl.), 518.
(2) Strange, R. E.; Kent, L. H. *Biochem. J.* **1959**, *71*, 333.
(3) Hoshino, O.; Zehavi, U.; Sinay, P.; Jeanloz, R. W. *J. Biol. Chem.* **1972**, *247*, 381.
(4) Lee, L.; Cherniak, R. *Carbohydr. Res.* **1974**, *33*, 387.
(5) Kenne, L.; Lindberg, B.; Lindqvist, B.; Lönngren, J.; Arie, B.; Brown, R. B.; Stewart, J. E. *Carbohydr. Res.* **1976**, *51*, 287.
(6) Dmitriev, B. A.; L'vov, L. V.; Kochetkov, N. K. *Carbohydr. Res.* **1977**, *56*, 207.
(7) Jansson, P.-E.; Lindberg, B.; Lönngren, J.; Ortega, C.; Nimmich, W. *Carbohydr. Res.* **1984**, *132*, 297.
(8) Kochetkov, N. K.; Dmitriev, B. A.; L'vov, L. V. *Carbohydr. Res.* **1977**, *54*, 253.
(9) Oxley, D.; Wilkinson, S. *Carbohydr. Res.* **1991**, *215*, 293.
(10) Severn, W. B.; Richards, J. C. *Carbohydr. Res.* **1990**, *206*, 311.
(11) Dmitriev, B. A.; Backinowsky, L. V.; Knirel, Yu. A.; Kochetkov, N. K.; Hofman, L. L. *Eur. J. Biochem.* **1977**, *78*, 381.
(12) Dmitriev, B. A.; Knirel, Yu. A.; Kochetkov, N. K.; Jann, B.; Jann, K. *Eur. J. Biochem.* **1977**, *79*, 111.
(13) Kochetkov, N. K.; Dmitriev, B. A.; Backinowsky, L. V. *Carbohydr. Res.* **1976**, *51*, 229.
(14) Kochetkov, N. K.; Sviridov, A. F.; Arifkhodzhaev, K. A.; Chizhov, O. S.; Shashkov, A. S. *Carbohydr. Res.* **1979**, *71*, 193.
(15) Severn, W. B.; Richards, J. C. *Can. J. Chem.* **1992**, *70*, 2664.
(16) Sviridov, A. F.; Arifkhodzhaev, Kh. A.; Shashkov, A. S.; Botvinko, I. V.; Chizhov, O. S.; Kochetkov, N. K. *Bioorg. Chem.* **1979**, *5*(*4*), 568.
(17) Lindberg, B.; Lindqvist, B.; Lönngren, J.; Nimmich, W. *Carbohydr. Res.* **1977**, *58*, 443.

0002-7863/93/1515-1114$04.00/0